Anchoring of protein kinase A-regulatory subunit II alpha to subapically positioned centrosomes mediates apical bile canalicular lumen development in response to oncostatin m but not cAMP

Wojtal, Kacper A.; Hoekstra, Dick; van Ijzendoorn, Sven C. D.

Published in:
Molecular Biology of the Cell

DOI:
10.1091/mbc.E06-08-0732

Publication date:
2007

Molecular Biology of the Cell
Vol. 18, 2745–2754, July 2007

Anchoring of Protein Kinase A-Regulatory Subunit IIα to Subapically Positioned Centrosomes Mediates Apical Bile Canalicular Lumen Development in Response to Oncostatin M but Not cAMP[D]

Kacper A. Wojtal, Dick Hoekstra, and Sven C.D. van IJzendoorn

Department of Cell Biology/Membrane Cell Biology, University Medical Center Groningen, University of Groningen, 9713 AV Groningen, The Netherlands

Submitted August 21, 2006; Revised April 19, 2007; Accepted May 1, 2007
Monitoring Editor: Ben Margolis

Oncostatin M and cAMP signaling stimulate apical surface-directed membrane trafficking and apical lumen development in hepatocytes, both in a protein kinase A (PKA)-dependent manner. Here, we show that oncostatin M, but not cAMP, promotes the A-kinase anchoring protein (AKAP)-dependent anchoring of the PKA regulatory subunit (R)IIα to subapical centrosomes and that this requires extracellular signal-regulated kinase 2 activation. Stable expression of the RII-displacing peptide AKAP-IS, but not a scrambled peptide, inhibits the association of RIIα with centrosomal AKAPs and results in the repositioning of the centrosome from a subapical to a perinuclear location. Concomitantly, common endosomes, but not apical recycling endosomes, are repositioned from a subapical to a perinuclear location, without significant effects on constitutive or oncostatin M-stimulated basolateral-to-apical transcytosis. Importantly, however, the expression of the AKAP-IS peptide completely blocks oncostatin M-, but not cAMP-stimulated apical lumen development. Together, the data suggest that centrosomal anchoring of RIIα and the interrelated subapical positioning of these centrosomes is required for oncostatin M-, but not cAMP-mediated, bile canalicular lumen development in a manner that is uncoupled from oncostatin M-stimulated apical lumen-directed membrane trafficking. The results also imply that multiple PKA-mediated signaling pathways control apical lumen development and that subapical centrosome positioning is important in some of these pathways.

INTRODUCTION

Polarized hepatocytes, like all epithelial cells, display distinct plasma membrane domains, an apical plasma membrane domain facing the bile canalicular lumen, and a basolateral plasma membrane domain facing the space of Disse. Concomitant with cell surface polarity, also the cell interior displays a polarized organization. A dense cortical actin network is assembled beneath the apical surface and actin filaments extend into apical microvilli with their barbed ends facing the microvilli tips. In addition, part of the microtubule cytoskeleton is oriented parallel to the apical–basolateral axis with their minus and plus ends facing the apical and basolateral surface, respectively. The cytoskeleton organization influences the position of the centrosome (Burakov *et al*., 2003), which in various epithelial cells including intestinal Caco-2, kidney Madin-Darby canine kidney (MDCK), and hepatic WIF-B cells, is typically oriented toward the apical surface (Buendia *et al*., 1990; Meads and Schroer, 1995; Salas, 1999). Polarized positioning of the centrosome is thought to play a role in the establishment of epithelial cell polarity (Zeligs, 1979; Dylewski and Keenan, 1984; Houliston *et al*., 1987; Rizzolo and Joshi, 1993) and neuronal polarity (de Anda *et al*., 2005; Higginbotham *et al*., 2006). A subapical position of the centrosome may be important for the polarized orientation of microtubule-associated organelles such as the Golgi apparatus and recycling endosomes, and, in this way, facilitate the polarized, at least apical, trafficking of proteins and lipids from these intracellular organelles to the appropriate surface domain (Wald *et al*., 2003; Musch, 2004). However, kidney epithelial MDCKII-J cells, which display a persistent perinuclear centrosome position and microtubule organization, do not show defects in polarity development or protein delivery from the Golgi apparatus to the different membrane domains, arguing for a nonessential role for centrosome position and microtubule organization in cell polarity development (Grindstaff *et al*., 1998). In the *Caenorhabditis elegans* oocyte, however, the centrosome is critical to initiate cell polarity but independent of its role as a microtubule nucleator. Here, the centrosome was proposed to provide a specific but unidentified polarity signal (Cowan and Hyman, 2004), which is in agreement with the emerging view of the centrosome as a signaling unit (for review, see Diviani and Scott, 2001; Lange, 2002). Whether the centrosome and its subcellular positioning play a general role in the development of (epithelial) cell polarity thus remains uncertain.

Hepatocyte polarity development is regulated by kinases, often in response to extracellular signals. For example, activation of the serine/threonine protein kinase C (PKC) in well-differentiated human hepatoma HepG2 cells or in iso-

This article was published online ahead of print in *MBC in Press* (http://www.molbiolcell.org/cgi/doi/10.1091/mbc.E06–08–0732) on May 9, 2007.

[D] The online version of this article contains supplemental material at *MBC Online* (http://www.molbiolcell.org).

Address correspondence to: Sven C.D. van IJzendoorn (s.c.d.van.ijzendoorn@med.umcg.nl).

lated rat hepatocyte couplets with phorbol esters or vasopressin, respectively, perturbs hepatocyte polarity and results in a loss of bile canalicular lumens and a redistribution of bile canalicular markers (Zegers and Hoekstra, 1997; Roma *et al*., 1998; Kubitz *et al*., 2001). By contrast, the mammalian orthologue of *Caenorhabditis elegans* Par-1 (EMK1; MARK2), which controls microtubule dynamics, is required for the development of apical bile canalicular lumens in rat hepatic WIF-B9 cells (Cohen *et al*., 2004). Phosphoinositide 3-kinase and the p38 mitogen-activated protein (MAP) kinase control tauro(ursodeoxy)cholate-induced trafficking of ATP-dependent transporters to the canalicular surface in rat liver, isolated hepatocytes, and hepatic cell lines (Misra *et al*., 1998; Sai *et al*., 1999; Kubitz *et al*., 2004), whereas Vps34p, a class III phosphoinositide 3-kinase, prevents the internalization of canalicular proteins from the canalicular surface (Tuma *et al*., 2001), in this way contributing to the functional composition of the apical lumen surface. Activation of cAMP-dependent serine/threonine protein kinase A (PKA) in WIF-B(9) cells, isolated hepatocyte couplets, or HepG2 cells with 1) forskolin, a compound produced by *Coleus forskohlii* that activates adenylyl cyclase to increase the intracellular levels of cAMP; 2) glucagon, a pancreatic hormone that similarly activates hepatic adenylyl cyclase to raise cAMP concentrations; 3) the cAMP phosphodiesterase inhibitor 3-isobutyl-1-methylxanthine, or 4) cell-permeable stable cAMP analogues generally stimulates the polarized delivery of apical bile canalicular proteins and lipids and the concomitant development of apical bile canalicular lumens (Zegers and Hoekstra, 1997; van IJzendoorn and Hoekstra, 1999; Roma *et al*., 2000; Kagawa *et al*., 2002; Gradilone *et al*., 2003). In addition, PKA protects hepatocytes against radical oxygen species-induced tight junction impairment (Perez *et al*., 2006), thus preserving separate apical and basolateral environments. Also, when freshly cultured HepG2 cells are exposed to the PKA inhibitor H89, further cell polarity development is prevented (van IJzendoorn and Hoekstra, 2000). The fundamental role of PKA in hepatocyte polarity development is underscored by the observation that basolaterally circulating oncostatin M (OSM), an interleukin-6 family cytokine involved in fetal liver maturation (Kamiya *et al*., 2001), stimulates membrane traffic toward the bile canalicular plasma membrane and bile canalicular lumen development in a PKA-dependent manner (van der Wouden *et al*., 2002).

How oncostatin M- and cAMP/PKA-mediated signaling routes intermingle is not known. Clearly, a coordinated spatial regulation of signaling within the cellular space is pivotal for a basolaterally localized stimulus to promote the development of an apical lumen, which are about ten microns apart. This is, for example, illustrated by the recruitment of the signal transducing receptor subunit gp130 into lipid rafts at the basolateral surface of HepG2 cells in response to oncostatin M (van der Wouden *et al*., 2002). As for PKA, there are two isoforms, PKA type I and type II, both of which are holoenzymes consisting of two regulatory (RIα/β or RIIα/β, respectively) and two catalytic subunits (C). The autoinhibitory interaction between R and C is relieved when cAMP, produced by adenylyl cyclase, binds to the regulatory subunits, triggering their dissociation from the catalytic subunits and subsequent phosphorylation of target proteins by C. In HepG2 and other cells, most PKA type II is anchored at specific organelles and cellular structures through A-kinase anchoring proteins (AKAPs), which, in conjunction with (phosphodiesterase-)regulated spatial cAMP gradients and other proteins tethered to AKAPs, provide an important level of control to ensure specificity of cAMP/PKA-mediated signal transduction (Michel and Scott, 2002). It has been shown that exposure of HepG2 cells to oncostatin M does not result in a detectable increase in cAMP levels or a pronounced increase in overall PKA activation, which is in striking contrast to treatment of the cells with forskolin or cAMP analogues. Intriguingly, however, it was noticed that oncostatin M signaling stimulated the association of the regulatory subunit of type II PKA (PKA-RIIα) with the centrosomal region (van der Wouden *et al*., 2002). In this study, we have examined the role of PKA-RIIα anchoring at centrosomes in hepatocyte polarity development.

MATERIALS AND METHODS

Cell Culture

Human hepatoma HepG2 cells (American Type Culture Collection, Manassas, VA) were grown in DMEM supplemented with L-glutamine, 10% fetal calf serum (FCS), and penicillin/streptavidin, as described previously (Zegers *et al*., 1997). HepG2 cells stably expressing the GFP/V5/His-tagged AKAP-IS peptide or scrambled peptide (GFP-QDVEIQLKAAYNQKLIAI-V5/His) (provided by John Scott (Howard Hughes Medical Institute, Vollum Institute, Oregon Health & Science University, Portland, OR 97239) and described in Alto *et al*. (2003)) were created as described previously (Wojtal *et al*., 2006). Stable transfectants were cultured in medium supplemented with 800 μg/ml Geneticin (G-418; Invitrogen, Carlsbad, CA). For immunofluorescence experiments, cells were plated onto ethanol-sterilized uncoated glass coverslips.

Determination of Cell Proliferation

Parental HepG2 and AKAP-IS–expressing HepG2 cells were plated at a concentration of 500,000 cells per coverslip (20 $\times$ 20 mm) and counted every 24 h using a Bürker chamber. The average of two different countings is depicted.

Flow Cytometry

Cells were washed with phosphate-buffered saline (PBS) and with PBS/0.1% EDTA, and incubated in PBS/0.1% EDTA at 37°C during 5 min. The cells were resuspended to obtain a single cell solution and centrifuged at 1000 rpm for 5 min. After washing with PBS/1% FCS, the cell pellet was resuspended in 100 μl of PBS. One milliliter of −20°C absolute ethanol was added using a vortex to avoid clumping, and cells were kept in ethanol at 4°C for 15 min and centrifuged at 1600 rpm for 5 min. After washing with PBS/FCS, the cells were suspended in a propidium iodide solution (10 μg/ml propidium iodide in 38 mM sodium citrate, pH 7. 4, 250 μg/ml RNase A in PBS/1% FCS) and incubated at 37°C for 30 min. The cells were stored in the fridge and protected from light until analysis with a FACSCalibur flow cytometry apparatus, using CellQuest software for the data acquisition and Modfit for the data analysis (BD Biosciences, San Jose, CA).

Determination of Cell Polarity

The evaluation of polarity was performed as described previously (Zegers *et al*., 1997; van IJzendoorn *et al*., 2000). Briefly, cells were plated onto coverslips, and after 72 h they were fixed with absolute ethanol (−20°C) for 10 s, washed with PBS, and subsequently incubated with a mixture of tetramethylrhodamine isothiocyanate (TRITC)-labeled phalloidin (100 ng/ml) and Hoechst-33528 (5 ng/ml) at room temperature (RT) for 30 min. The coverslips were then washed with PBS and mounted. The level of polarity was determined by counting of the number of TRITC–phalloidin-positive bile canaliculi (BC) per 100 cells, and level is expressed in percentage. At least 10 fields each containing >300 cells were counted using an epifluorescence microscope (Provis AX70; Olympus, New Hyde Park, NY).

Immunofluorescence Labeling of Cells

For centrosomal staining, cells were treated with cold Hanks' balanced salt solution (HBSS) containing Triton X-100 (1%, vol/vol) for 2 min at 4°C and immediately fixed with −20°C absolute methanol for 10 min at −20°C. Cells were then washed with PBS and blocked with bovine serum albumin (BSA) (1%, wt/vol) in HBSS for 1 h at RT. Cells were incubated with mouse monoclonal anti-PKA-RIIα (BD Biosciences Transduction Laboratories, Lexington, KY), rabbit polyclonal anti-γ-tubulin (Sigma-Aldrich, St. Louis, MO), and/or rabbit anti-pericentrin (Covance, Princeton, NJ) primary antibodies for 2 h at RT or alternatively overnight at 4°C. For staining of microtubules and apical recycling endosomes (AREs), cells were fixed with paraformaldehyde (4%, wt/vol) and permeabilized with Triton X-100 (0.1%, vol/vol) and subsequently incubated with mouse anti-β-tubulin (Sigma-Aldrich) or rabbit anti-rab11a (Zymed Laboratories, South San Francisco, CA) antibodies, respectively. The cells were then washed and incubated with the corresponding secondary antibodies labeled with either Alexa Fluor-488 or -594 (Invitrogen)

for 1 h at RT and 5 ng/ml Hoechst to stain the nuclei or TRITC-phalloidin (Sigma-Aldrich) to stain apical actin cytoskeleton to visualize BCs. The coverslips were mounted and analyzed by epifluorescence microscopy (Provis AX70; Olympus).

Quantification of PKA-RIIα–positive Centrosomes

The percentage of PKA-RIIα–positive centrosomes was determined by counting the number of γ-tubulin–stained centrosomes that were positive or negative for PKA-RIIα. The number of PKA-RIIα–positive centrosomes was expressed as the percentage of total number of centrosomes. Several fields of several coverslips were analyzed.

Cell Lysis, Protein Determination, and Trichloroacetic Acid (TCA) Precipitation

Cells were scraped in ice-cold NP-40 lysis buffer, pH 7.4, supplemented with a cocktail of protease inhibitors. An homogenous lysate was obtained by resuspending the cells through the 24-gauge needle. Ten microliters of lysate was processed for protein determination using bicinchoninic acid and $CuSO_4$ method. Equal amounts of proteins were precipitated by TCA. Briefly, samples containing equal amount of proteins were complemented until a total volume of 1 ml with fractionation buffer (supplemented with a cocktail of protease inhibitors) was reached. Afterward, 5 μl of 25 mg/ml deoxycholic acid was added to each sample and incubated on ice for 5 min. Proteins were then precipitated by adding 60 μl of 100% TCA followed by 15-min incubation on ice. Proteins were pelleted at 10,000 × rpm at 4°C for 20 min, after which the pellet was dried under vacuum, resuspended in sample buffer containing SDS (2%, wt/vol), 1% β-mercaptoethanol, 10% glycerol, 50 mM Tris, pH 6.8, and 0.02% bromophenol blue (BFB), and boiled for 4 min.

SDS-Polyacrylamide Gel Electrophoresis (PAGE) and Western Blotting

Protein samples were separated with SDS-PAGE 10% acrylamide and subsequently transferred to polyvinylidene difluoride (PVDF) or nitrocellulose membranes. Membranes were blocked with 5% nonfat dry milk in PBS-Tween 20 (0.3%, vol/vol) and incubated with monoclonal anti-PKA RIIα (BD Biosciences Transduction Laboratories), monoclonal mouse anti- β-actin (Sigma-Aldrich), or goat polyclonal anti-PKA-RII (Upstate Biotechnology, Lake Placid, NY) antibodies at room temperature for 2 h. For total expression of PKA-RIIα and AKAP350, membranes were incubated with mouse monoclonal anti-PKA-RIIα antibody (BD Biosciences Transduction Laboratories) or mouse anti-AKAP350 antibody (gift from Dr. Goldenring, Vanderbilt University, School of Medicine, Nashville, TN 37232) for 2 h at RT in PBS containing 0.1% Tween. For phosphorylation of extracellular signal-regulated kinase (ERK)1/2, cells were lysed as described above, and 30 μg of total protein was suspended in sample buffer containing 2% SDS, 1% β-mercaptoethanol, 10% glycerol, 50 mM Tris, pH 6.8, and 0.02% BFB, boiled for 4 min, and processed for SDS-PAGE and transferred onto nitrocellulose or PVDF membranes. After transfer, membranes were blocked with 5% nonfat dry milk in Tris-buffered saline (TBS) (+1%, vol/vol Tween) and incubated overnight at 4°C with rabbit anti-p44/p42 MAP kinase or mouse anti-phospho-p44/p42 MAP kinase antibodies (Cell Signaling Technology, Danvers, MA), or mouse anti-p27Kip1 (BD Biosciences, Transduction Laboratories) antibodies in TBS containing 5% (wt/vol) BSA. Membranes were then washed three times for 5 min with PBS-Tween 20 (0.3%, vol/vol) and incubated with corresponding secondary horseradish peroxidase-conjugated antibodies (GE Healthcare, Little Chalfont, Buckinghamshire, United Kingdom) at room temperature for 1 h and processed for enhanced chemiluminescence detection (GE Healthcare). Bands were quantified using free Scion Imaging software (Scion, Frederick, MD; www.scioncorp.com).

Quantification of Expression of Pericentrin

HepG2 cells were plated onto glass coverslips, and after 72 h, they were subjected to treatment with 10 ng/ml OSM or 1 mM dibutyryl (db)-cAMP for 4 h. Cells were then fixed with cold methanol at −20°C for 10 min. After blocking with 1% of BSA in PBS for 1 h at RT, coverslips were incubated with primary rabbit anti-pericentrin antibody (Covance) overnight at 4°C. After washing three times with PBS, coverslips were probed with corresponding anti-rabbit Alexa-594 (Invitrogen) at RT for 1 h. Coverslips were mounted and processed for fluorescence microscopy (Provis AX70; Olympus) by using 60× objective. Several images were taken from different fields of each coverslip using analySIS (Soft Imaging Systems, Münster, Germany) at 1-s exposure time, and all other used software settings were standardized for accurate comparison between images. The intensity of fluorescence was measured by free Scion Imaging software.

Synthesis of C_6-Nitro-benzoxa-diazole (C_6-NBD)-Sphingomyelin

C_6-NBD-sphingomyelin (SM) was synthesized from C_6-NBD and sphingosylphosphorylcholine as described previously (van der Wouden *et al*., 2002). The C_6-NBD-SM was stored at −20°C and routinely checked for purity.

Transcytosis of Sphingolipids

HepG2 cells expressing the AKAP-IS peptide or not were washed three times in HBSS and preincubated for 30 min at 37°C in HBSS supplemented or not with 10 ng/ml OSM. After the preincubation, the cells were cooled to 4°C by washing with ice-cold HBSS. Subsequently, the basolateral plasma membrane (PM) was labeled with 4 μM C_6-NBD-SM for 30 min at 4°C in HBSS supplemented or not with OSM, which allows incorporation of the lipid probe in the exoplasmic leaflet of the basolateral plasma membrane while preventing its internalization (van IJzendoorn *et al*., 1997). When cells had been pretreated with OSM, the cytokine was included in all further incubations. After incorporation of the lipid probe in the basolateral plasma membrane, cells were washed, and transcytosis was allowed to occur at 37°C for different time periods. To terminate transport, the cells were cooled by washing three times with ice-cold HBSS, and lipid remaining in the outer leaflet of the basolateral membrane was removed by a back-exchange procedure. To this end, the cells were incubated for 30 min at 4°C with 5% BSA in HBSS, followed by washing with ice-cold HBSS. This procedure was repeated once (van IJzendoorn *et al*., 1997).

Labeling of the CE/SAC with Fluorescent Lipid Analogues

The CE/SAC was labeled with the lipid analogue exactly as described in detail previously (van IJzendoorn and Hoekstra, 1998, 1999). In brief, cells were labeled with 4 μM C_6-NBD-SM at 37°C to allow internalization from the basolateral surface and subsequent transcytosis to the apical, BC PM domain. After 30 min of incubation, lipid analogue still residing at the basolateral domain was depleted by a back-exchange procedure at 4°C (2 × 30-min incubation in HBSS + 5%, wt/vol BSA; compare with van IJzendoorn *et al*., 1997), and BC-associated lipid analogue was chased into the SAC at 18°C for 1 h in back-exchange medium. Then, the NBD fluorescence at the exoplasmic leaflet of the bile canalicular plasma membrane was destroyed using sodium dithionite at 4°C, leaving the majority of the lipid probe-derived fluorescence in the SAC (van IJzendoorn and Hoekstra, 1998, 2000).

RESULTS

OSM but Not Dibutyryl-cAMP Stimulates the Association of PKA-RIIα with Centrosomes

In a previous study, we observed that OSM-stimulated and PKA-dependent apical lumen development in HepG2 cells coincided with an increased localization of PKA-RIIα at the centrosomal region (van der Wouden *et al*., 2002). To investigate this in more detail, cells were treated with 10 ng/ml human recombinant OSM or buffer (control) in the extracellular medium at 37°C for 4 h, fixed, and immunolabeled with mouse monoclonal antibodies against PKA-RIIα and rabbit polyclonal antibodies against the centrosomal protein γ-tubulin. In untreated HepG2 cells in interphase, typically one γ-tubulin–positive centrosome consisting of two centrioles was observed per cell (Figure 1A). In polarized cells, on average 2.3 ± 0.2 centrosomes, identified by γ-tubulin staining, were counted within a 2-μm distance from each apical surface (BC; Figure 2A), consistent with the participation of typically two to three cells per apical lumen (cf. Herrema *et al*., 2006). Most centrosomes are therefore subapically positioned in polarized cells (Figure 1, A–C, merged image in D). There were no differences in γ-tubulin staining between nontreated and OSM-treated cells (cf. Figure 1, A–D), and identical results were obtained with antibodies against pericentrin (data not shown).

Immunofluorescence microscopy revealed the presence of PKA-RIIα in the cytosol, in the nucleus, and at the centrosome (Figure 1, A′ and B′). Centrosomal PKA-RIIα seemed to localize at the pericentriolar material surrounding and partially overlapping with the individual pericentrin-positive centrioles (Figure 1, E–G), which is in accordance with the localization of PKA anchoring proteins such as AKAP350 and pericentrin at the pericentriolar material (Keryer *et al*., 1993; Doxsey *et al*., 1994). The percentage of PKA-RIIα–containing centrosomes was determined by counting centrosomes, identified by γ-tubulin staining, that were positive for PKA-RIIα. In untreated cells, PKA-RIIα was detected at ~48% of the (γ-tubulin–positive) centrosomes (Figure 2B). The majority of the centrosomes that seemed devoid of PKA-RIIα was found in interphase cells

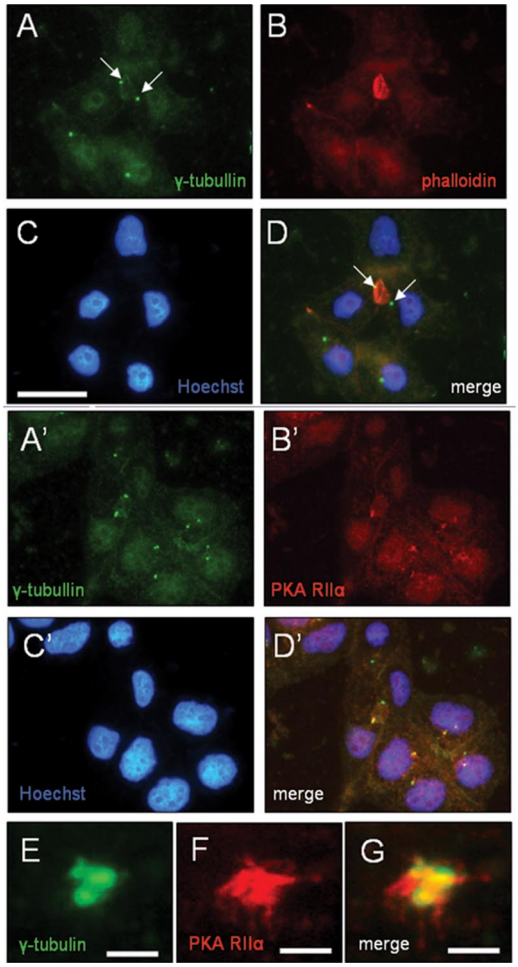

Figure 1. Localization of centrosomes in polarized HepG2 cells. Seventy-two hours after plating, HepG2 cells were stained with anti-γ-tubulin antibody to visualize centrosomes (A) and TRITC-phalloidin to stain apical surfaces (B). In polarized cells, most centrosomes (arrows) localize at the apical surface (D), some of which are positive for PKA-RIIα as shown in the bottom panel (A′, B′, and D′). Nuclei were stained with Hoechst (C and C′). (E–G) A close-up shows that PKA-RIIα (F) is localized at the pericentriolar mesh, surrounding and partially overlapping with the pericentrin-positive centrioles (E). Merged image in G. Bars, 20 μm (A–D′) and 0.5 μm (E–G).

(evidenced by DNA staining), and a minor fraction (~4%) was found in mitotic cells, the latter of which never showed PKA-RIIα at the centrosome (our unpublished data). The percentage of γ-tubulin–positive centrosomes that harbored PKA-RIIα increased to ~65% in OSM-treated cells ($p < 0.01$; Student's *t* test) (Figure 2B). Determination of the percentage of centrosomes containing PKA-RIIα that are within a 2-μm distance from an apical lumen showed an increase from an average of 1.0–1.4 per lumen ($p < 0.05$) in nontreated and OSM-treated cells, respectively (Figure 2C), whereas the percentage of total centrosomes (i.e., irrespective of PKA-RIIα association) within a 2-μm distance of an apical lumen remained constant at an average of ~2.3 per lumen (Figure 2A). These data suggest that OSM stimulates the association of PKA-RIIα with already subapical centrosomes.

Both OSM and PKA positivity of centrosomes have been correlated to cell entry in or exit out of the G1 phase of the cell cycle. We therefore examined the expression level of p27Kip1 (a cyclin-dependent kinase inhibitor that controls G1 progression, which typically changes as a function of cell cycle progression). However, during the relatively short time interval of incubation with OSM, no changes in the expression level of p27Kip1 were observed (Supplemental Figure S1A). The stimulatory effect of OSM on the association of PKA-RIIα with centrosomes therefore is unlikely the result of changes in cell cycle.

OSM-elicited signaling cascades involve, among others, the p42 MAP kinase/ERK2, which becomes phosphorylated upon treatment of the cells with OSM (Figure 2D), in agreement with previous reports (Klausen *et al*., 2000). Treatment of the cells with PD98059, a compound that binds to the ERK-specific MAP kinase kinase (MEK) and in this way prevents phosphorylation of ERK by MEK, prevented the OSM-stimulated phosphorylation of ERK2 (Figure 2D) and inhibited the OSM-stimulated association of PKA-RIIα with centrosomes (Figure 2B). This suggests that the enhanced association of PKA-RIIα with centrosomes in response to OSM requires the OSM-mediated activation of ERK2 via MEK.

In contrast to OSM, treatment of HepG2 cells with the membrane-permeable and stable cAMP analogue db-cAMP at 1 mM, which effectively stimulates PKA activity in HepG2 (van der Wouden *et al*., 2002) and other cells, did not stimulate the association of PKA-RIIα with centrosomes (Figure 2B). Note that the cellular expression level of PKA-RIIα and two known centrosomal AKAPs, pericentrin and AKAP350 (a.k.a. AKAP450 or CG-NAP), did not change upon treatment of the cells with OSM or db-cAMP, as evidenced by Western blot (RIIα and AKAP350; Figure 2E) or quantitative immunofluorescence (pericentrin, Figure 2F), suggesting that the OSM-enhanced association of PKA-RIIα with centrosomes reflected a redistribution of the protein rather than an increase in expression.

To determine whether the catalytic activity of PKA was required for the OSM-stimulated association of PKA-RIIα with centrosomes, cells were treated with OSM in combination with the ATP-site PKA inhibitors H89 or KT5720. These structurally different inhibitors were shown in our laboratory to effectively inhibit cAMP-stimulated development of apical lumens in HepG2 cells (Zegers and Hoekstra, 1997; van IJzendoorn and Hoekstra, 1999, 2000; Supplemental Figure S2). As shown in Figure 2B, H89 and KT5720 did not interfere with the OSM-stimulated association of PKA-RIIα with centrosomes, suggesting that catalytic activity of PKA is not required.

Together, the data show that in HepG2 cells, robust PKA-RIIα staining is detected at 48% of (γ-tubulin–positive) centrosomes and that treatment of the cells with OSM, but not db-cAMP, causes a significant MEK–ERK2-dependent increase in the association of PKA-RIIα at centrosomes.

Inhibition of PKA-RIIα Anchoring at Centrosomes Interferes with the Subcellular Positioning of the Centrosome and Common Endosome

To confirm that the OSM-stimulated association of PKA-RIIα with centrosomes occurs via an AKAP, and to investigate whether the OSM-stimulated association of PKA-RIIα with centrosomes plays a role in OSM-stimulated bile canalicular lumen development (van der Wouden *et al*., 2002; van IJzendoorn *et al*., 2004a), HepG2 cells were stably transfected with epitope-tagged AKAP-IS, a peptide that specifically binds to PKA-RII with high affinity and displaces it from its natural anchoring sites, or, as a control, stably transfected with an epitope-tagged nonfunctional scrambled peptide (details with regard to these peptides are described

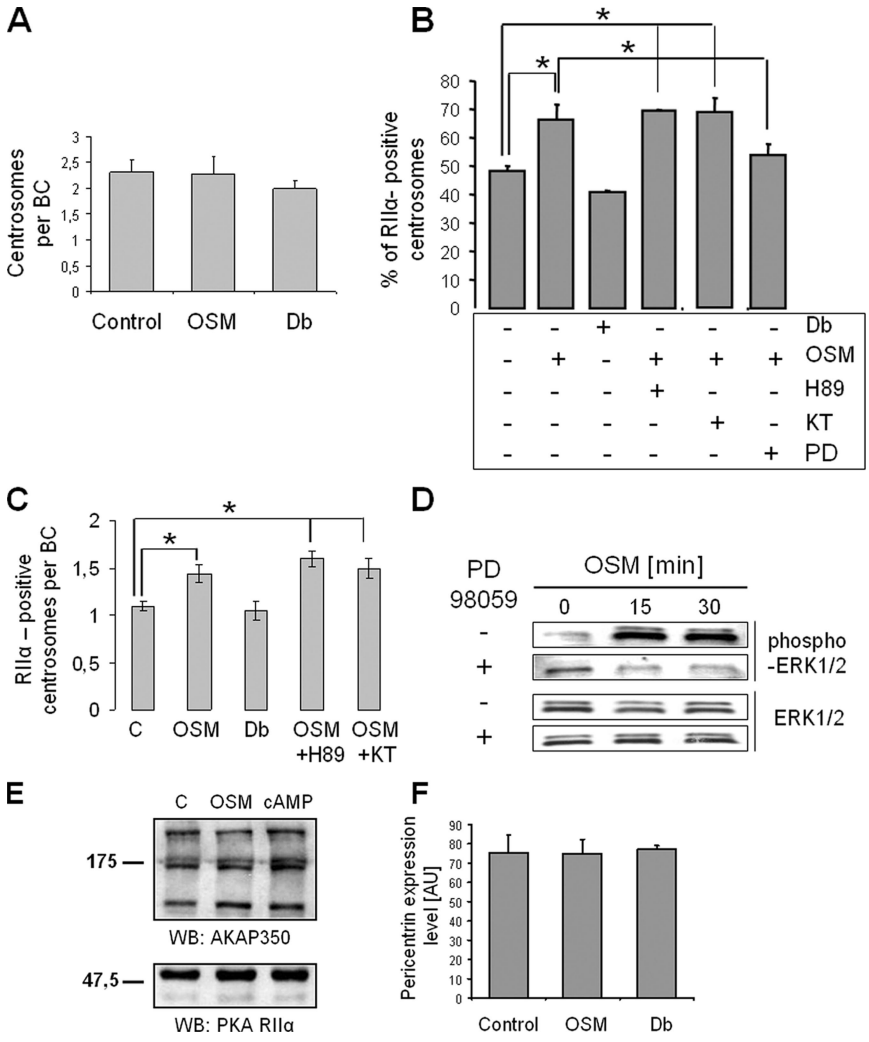

Figure 2. OSM promotes the association of PKA-RIIα with subapically positioned centrosomes. (A) Polarized HepG2 cells were treated at 37°C for 4 h with 10 ng/ml OSM or 1 mM db-cAMP. Cells were then fixed and immunolabeled for γ-tubulin and labeled with TRITC-phalloidin to determine the number of centrosomes positioned within a 2-μm radius from the apical surface. (B) OSM stimulates the recruitment of PKA-RIIα at the centrosomes in an ERK-, but not PKA-dependent manner. HepG2 cells were treated with db-cAMP or OSM at 37°C for 4 h. In other experiments, cells were treated with OSM in the presence of the MEK inhibitor PD98059 at 50 μM, or with the PKA inhibitors KT5720 at 10 μM or H89 at 10 μM. Cells were then fixed and immunolabeled for PKA-RIIα and γ-tubulin to determine the number of PKA-RIIα–positive centrosomes. (C) Cells were stimulated with OSM in the presence of absence of KT-5720, or H89 or db-cAMP, fixed, and (immuno)labeled for PKA-RIIα and TRITC-phalloidin to determine the number of PKA-RIIα–positive centrosomes within a 2-μm radius from the apical lumen. (D) PD98059 at 50 μM blocks the OSM-stimulated phosphorylation of ERK1/2, evidenced by Western blotting. (E) Western blot showing the expression level of AKAP350 and PKA-RIIα in untreated HepG2 cells and cells treated with 10 ng/ml OSM or 1 mM db-cAMP at 37°C for 4 h. (F) Quantification of the cellular expression of pericentrin in untreated cells and cells treated with OSM or db-cAMP. Quantification was based on the measured fluorescence intensity of immunolabeled coverslips (see *Materials and Methods*). All data are expressed as mean ± SD of at least three independent experiments. Statistical significance ($p < 0.05$; indicated with asterisks) was determined using a Student's *t* test.

in Alto *et al*., 2003). Stable transfectants were selected, and they were shown to express AKAP-IS or the scrambled peptide and displace PKA-RIIα from natural anchoring sites or not, respectively (cf. Wojtal *et al*., 2006). In cells stably expressing the AKAP-IS peptide, but not the scrambled peptide, the percentage of PKA-RIIα–positive centrosomes (identified by γ-tubulin) was significantly reduced (Figure 3A). The expression level of PKA-RIIα in cells expressing the peptide was not changed compared with parental HepG2 cells (cf. Wojtal *et al*., 2006). Importantly, in contrast to parental HepG2 cells or HepG2 cells expressing the scrambled peptide, treatment of cells expressing the AKAP-IS peptide with OSM at 37°C for 4 h did not result in an increase in the percentage of centrosomes that contained PKA-RIIα (Figure 3A), confirming that OSM stimulated the association of PKA-RIIα with centrosomes in parental HepG2 cells by promoting its AKAP-mediated anchoring. Expression of the AKAP-IS peptide did not prevent the OSM-stimulated phosphorylation of ERK2 (Figure 3B). Together, the data suggest that expression of the AKAP-IS peptide reduces the anchoring of PKA-RIIα to centrosomes, and, importantly, that it effectively prevents the OSM-stimulated association of PKA-RIIα with centrosomes.

Interestingly, we noticed that many centrosomes were no longer positioned near the apical surface in cells expressing the AKAP-IS peptide (Figure 3C, 2–4, compare with 1–3; cf. Figure 1, A–D). Indeed, on average no more than 0.5 PKA-RIIα-positive and 1.2 γ-tubulin positive centrosomes per apical lumen were counted, which is in striking contrast to the typically 1.0 PKA-RIIα-positive and 2.3 γ-tubulin–positive centrosomes per apical lumen in parental HepG2 cells or HepG2 cells expressing the scrambled peptide (Figure 3, D and E). The number of cells participating in an apical lumen did not change (data not shown). PKA-RIIα- and γ-tubulin–positive centrosomes were localized in proximity to the nucleus (Figure 3C, 2–4). Inhibition of catalytic PKA activity with KT5720 or H89 for 4 h did not result in a relocation of subapical centrosomes in parental HepG2 cells (Figure 2B), suggesting that the observed loss of subapical positioning in cells expressing the AKAP-IS peptide occurred independently of altered PKA activity. The perinuclear position of the centrosome in AKAP-IS–expressing cells altered the overall organization of the microtubule network, as many microtubules were concentrated in the perinuclear region away from the apical surface (Figure 3C, 4). Microtubules that seemed to be directed toward the apical domain were also observed (Figure 3C, 5). These data suggest that expression of the AKAP-IS peptide and concomitant reduction of centrosome-associated PKA-RIIα interferes with the subapical positioning of the centrosome and the orientation of a major part of the microtubule net-

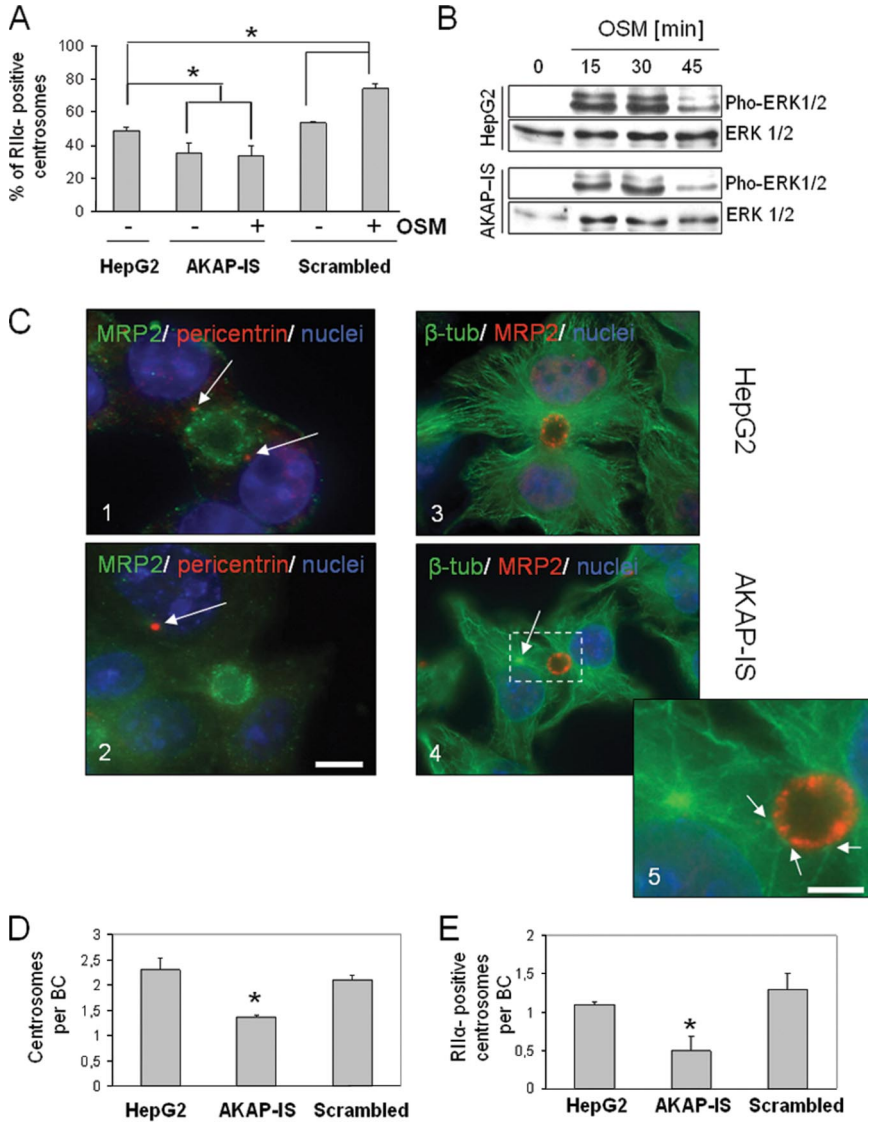

Figure 3. In HepG2 cells stably expressing AKAP-IS peptide centrosomes are positioned away from apical plasma membranes. (A). Parental HepG2 cells or HepG2 cells expressing the AKAP-IS or scrambled (control) peptide were treated with OSM or buffer (control) at 37°C for 4 h and immunolabeled for γ-tubulin and PKA-RIIα to determine the number of PKA-RIIα–positive centrosomes. Note that in cells expressing the AKAP-IS peptide, the association of PKA-RIIα with centrosomes is decreased and OSM is not able to stimulate the anchoring of PKA RIIα to centrosomes. Data are expressed as mean ± SD from three independent experiments. (B) Western blot showing phosphorylated ERK1/2 and total ERK1/2 in HepG2 cells and HepG2 cells expressing the AKAP-IS peptide treated for the indicated time intervals with OSM. (C) HepG2 cells (1 and 3) or HepG2 cells expressing the AKAP-IS peptide (2, 4, and 5) were immunolabeled for MRP2 and β-tubulin (3–5) or MRP2 and pericentrin (1 and 2). Note that in polarized HepG2 cells stably expressing AKAP-IS peptide, centrosomes (arrows) and the microtubule network are perinuclearly oriented. Image 5 is an enlargement of the boxed region in image 4. (E) HepG2 cells or HepG2 cells expressing the AKAP-IS or scrambled peptide were (immuno)labeled for γ-tubulin and TRITC-phalloidin to determine the number of centrosomes within a 2-μm radius from the apical surface. (F) HepG2 cells or HepG2 cells expressing the AKAP-IS or scrambled peptide were (immuno)labeled for PKA-RIIα and TRITC-phalloidin to determine the number of RIIα-positive centrosomes within a 2-μm radius of the apical surface. Data are expressed as mean ± SD from three independent experiments. Statistical significance was determined using a Student's *t* test. Bar, 10 μm.

work in a manner that seems unrelated to the enzymatic activity of PKA.

Several endosomal compartments such as the CE/SAC and the rab11a-positive ARE are typically concentrated around the centrosome in epithelial cells (Casanova *et al.*, 1999; Leung *et al.*, 2000; Hobdy-Henderson *et al.*, 2003), and they mediate the transcellular flow of membranes (for review, see Hoekstra *et al.*, 2004), a process that has been shown to be stimulated by OSM (van der Wouden *et al.*, 2002). Therefore, we next examined the subcellular position of the CE/SAC and ARE in control HepG2 cells and HepG2 cells expressing the AKAP-IS peptide. The CE/SAC was visualized by the temperature-dependent accumulation of a fluorescent lipid probe, as described previously (van IJzendoorn and Hoekstra, 1998). In brief, cells were labeled with NBD-sphingomyelin at 37°C for 30 min, washed, and incubated at 18°C for another 90 min in buffer containing 5% (wt/vol) albumin. Cells were then treated with dithionite at 4°C for 10 min, washed once with buffer, and examined with epifluorescence microscopy. As shown in Figure 4, A and B, CE/SAC (open arrows) were oriented toward the apical surfaces (closed arrow) in HepG2 cells, consistent with previous results (van IJzendoorn and Hoekstra, 1998, 1999, 2000; van IJzendoorn *et al.*, 2004a,b). In contrast, in HepG2 cells expressing the AKAP-IS peptide, many CE/SAC (open arrows) were no longer oriented toward the apical surface (closed arrow), and they displayed a perinuclear localization (Figure 4, C and D), in accordance with the position of the centrosome in these cells (cf. Figure 3C, 2–5). The ARE was visualized using an antibody raised against rab11a, a well-established ARE-associated small GTPase (Casanova *et al.*, 1999; Brown *et al.*, 2000; Leung *et al.*, 2000; Prekeris *et al.*, 2000). In parental HepG2 cells, rab11a labeling was exclusively subapical, as expected (Figure 4, F and G). In HepG2 cells expressing the AKAP-IS peptide, the subapical rab11a labeling was preserved. In addition to the subapical labeling, however, in these cells rab11a labeling could also be observed at the perinuclear centrosomes (Figure 4, J and K, closed arrows). Together, these data show that the displacement of PKA-RIIα from centrosomes and the concomitant positioning of centrosomes away from the apical surface spatially separates the CE/SAC from rab11a-positive ARE, and they suggest that rab11a localizes to a separatable subapical and centrosomal pool.

Because (loss of) PKA-RII association with centrosomes has been correlated to cell cycle progression, we examined the cell proliferation rate, mitotic index, and cell cycle dis-

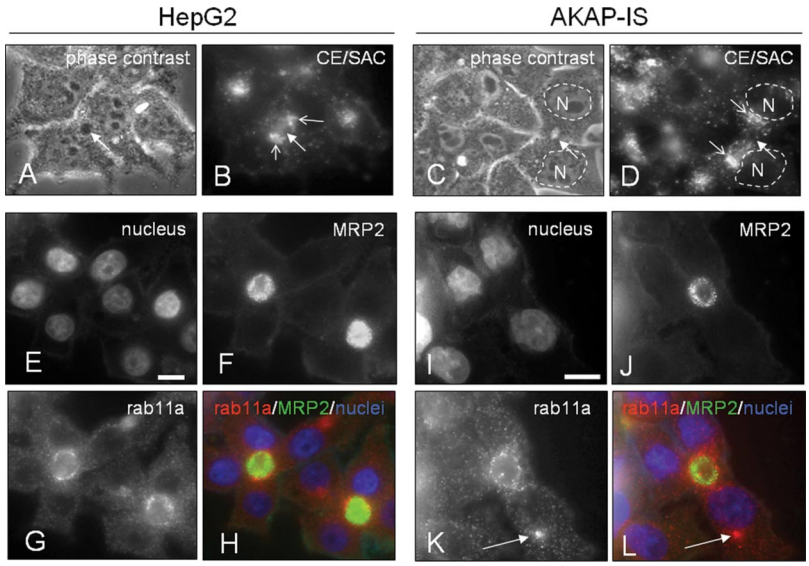

Figure 4. Subcellular distribution of the CE/SAC and ARE in HepG2 cells expressing the AKAP-IS peptide. The CE/SAC (A–D, open arrows; fluorescently labeled as described in *Materials and Methods*) are located close to the apical lumen (marked with closed arrow) in HepG2 cells (B; corresponding phase contrast in A, respectively). In cells expressing the AKAP-IS peptide, the CE/SAC (D, open arrows) is oriented away from the apical surface (corresponding phase contrast in C). In HepG2 cells, the rab11a-positive ARE (G) remains close to the apical surface (F and H). In HepG2 cells expressing the AKAP-IS peptide, rab11a (K) is also located close to the apical surface (J and L), whereas some immunoreactivity is observed at perinuclear structures reminiscent of centrosomes (K and L, arrows). Nuclei in E and I are stained with 4,6-diamidino-2-phenylindole. Bar, 10 μm.

tribution of parental and AKAP-IS–expressing cells. The proliferation rates, the mitotic index (i.e., percentage of cells showing typical mitotic DNA figures), and the cell cycle distribution (measured by fluorescence-activated cell sorting [FACS]) of parental and AKAP-IS–expressing cells were comparable (Supplemental Figure S1, B–D), suggesting that the effects of AKAP-IS expression on centrosome and CE/SAC positioning are not likely due to changes in cell cycle.

Expression of the PKA-displacing AKAP-IS Peptide Inhibits OSM- but Not db-cAMP-stimulated Bile Canalicular Lumen Development

Because the expression of the AKAP-IS peptide prevented the OSM-stimulated association of PKA-RIIα with centrosomes (Figure 3A), we next examined whether expression of the AKAP-IS peptide also prevented the previously reported (van der Wouden *et al*., 2002; van IJzendoorn *et al*., 2004a) stimulation of apical bile canalicular lumen development, i.e., cell polarity, by OSM. For this, AKAP-IS–expressing and control HepG2 cells (i.e., parental cells or HepG2 cells expressing the scrambled peptide) were treated with OSM or buffer (control) at 37°C for 4 h, fixed, and labeled with TRITC-conjugated phalloidin to identify BC and the nuclear stain Hoechst. Cells were then examined with epifluorescence microscopy, and the ratio bile canalicular lumens (BC)/100 cells, as a measure for cell polarity (see *Materials and Methods*; cf. Zegers and Hoekstra, 1997; van IJzendoorn and Hoekstra, 2000), was determined. In both AKAP-IS–expressing and control HepG2 cells the ratio BC/100 cells was ~15 (Figure 5), which, when taken into account that at least two cells participate in a single BC, means that at least 30% of the cells in the culture were polarized. Treatment of parental HepG2 cells or HepG2 cells expressing the scrambled peptide with OSM stimulated the number of apical lumens with ~30% ($p < 0.05$) (Figure 5), consistent with previous results (van der Wouden *et al*., 2002; van IJzendoorn *et al*., 2004a). Also, db-cAMP stimulated apical lumen development, evidenced by an increase in their numbers and circumference (Figure 5). Treatment of HepG2 cells or HepG2 cells expressing the scrambled peptide with both OSM and db-cAMP augmented the increase in BC numbers (Figure 5). In striking contrast, treatment of cells expressing the AKAP-IS peptide with OSM resulted in a 40% decrease in cell polarity (Figure 5), whereas db-cAMP stimulated apical lumen development in these cells equally well as in the parental cells (Figure 5). Treatment with both OSM and db-cAMP resulted in a significant increase in BC numbers but to a lesser extent in comparison with treatment with db-cAMP alone (Figure 5). These data indicate that OSM (but not db-cAMP) is unable to stimulate apical lumen development in AKAP-IS–expressing cells, and, moreover, causes a loss of preexisting apical surface domains. Hence, the capacity of OSM to stimulate the anchoring of PKA-RIIα to centrosomes is functionally correlated to its control over apical lumen development.

Expression of the PKA-displacing AKAP-IS Peptide Does Not Inhibit OSM-stimulated Basolateral to Apical Transcytosis

The stimulatory effect of OSM on apical lumen development in HepG2 cells was previously shown to correlate with a

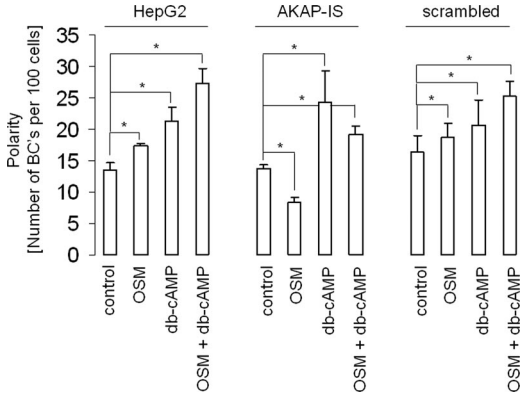

Figure 5. Displacement of PKA RIIα form its natural anchoring sites inhibits OSM-stimulated polarity development. Stimulation of parental HepG2 cells or HepG2 cells expressing the scrambled control peptide with either 10 ng/ml OSM, 1 mM db-AMP, or OSM + db-cAMP for 4 h stimulates the development of apical lumens. Expression of AKAP-IS peptide abrogates OSM-, but not db-cAMP-mediated stimulation of polarity. Data are expressed as mean ± SD from three independent experiments. Statistical significance was determined using a Student's *t* test.

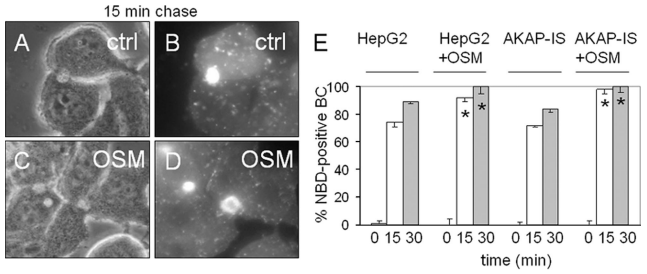

Figure 6. Basolateral-to-apical transcytosis of C_6-NBD-SM is stimulated in OSM-treated HepG2 cells that express or do not express the AKAP-IS peptide. HepG2 cells expressing the AKAP-IS peptide or not were labeled with 4 μM C_6-NBD-SM for 30 min at 4°C. Subsequently, the cells were washed and incubated with or without OSM for another 30 min at 4°C. Transport was triggered in the presence or absence of OSM by incubating the cells at 37°C. A–D show that the lipid analogue readily reaches the apical surface of (OSM-treated) cells expressing the AKAP-IS peptide, very similar to control HepG2 cells (cf. van der Wouden *et al*., 2002). After different time intervals, cells were cooled to block transport, and the number of NBD-positive BCs was determined (E). Data are expressed as mean ± SD from three independent experiments. Statistical significance was determined using a Student's *t* test.

stimulatory effect of the cytokine on basolateral-to-apical membrane trafficking, evidenced by an increased transcytosis of the fluorescent lipid analogue NBD-sphingomyelin (van der Wouden *et al*., 2002). Therefore, we next examined whether OSM could stimulate basolateral-to-apical membrane trafficking in cells expressing the AKAP-IS peptide. For this, cells cultured on glass coverslips were labeled with NBD-sphingomyelin as described previously (van der Wouden *et al*., 2002). In brief, control cells or cells expressing the AKAP-IS peptide were preincubated with OSM for 30 min, and the basolateral surface was incubated with NBD-sphingomyelin for 30 min at 4°C in the presence or absence of OSM. Cells were then washed and the fluorescent lipid analogue was chased at 37°C for 15 or 30 min in buffer in the presence or absence of OSM. Finally, cells were washed with ice-cold HBSS to stop membrane flow and the coverslips were mounted for immediate microscopy. Bile canalicular lumens were first identified with phase contrast and scored as NBD positive or negative with epifluorescence. Figure 6, A–D, shows that the lipid analogue reached the apical surface domain in untreated or OSM-treated cells expressing the AKAP-IS peptide, similarly as previously shown in control HepG2 cells (Zegers and Hoekstra, 1997; van IJzendoorn and Hoekstra, 1999, 2000; van der Wouden *et al*., 2002) and consistent with previous results (Wojtal *et al*., 2006). Basolaterally derived NBD-sphingomyelin reached 74 and 89% of the bile canalicular lumens after a chase of 15 and 30 min, respectively, in parental cells. Interestingly, treatment of both control and AKAP-IS–expressing cells with OSM stimulated basolateral to apical membrane trafficking as evidenced by an increase in the percentage of NBD-positive lumens after a 15- and 30-min chase to 92 and 100%, respectively (Figure 6E). These data show that, whereas OSM decreases the number of apical lumens in cells expressing the AKAP-IS peptide (cf. Figure 3), OSM is still capable of promoting transcytotic membrane trafficking to the remaining apical surfaces, and, therefore, strongly suggest that the OSM-stimulated loss of apical lumens in AKAP-IS–expressing cells cannot be attributed to an inhibition of apical surface-directed membrane trafficking.

DISCUSSION

The present study demonstrates that PKA-RIIα anchoring at the centrosome and the coinciding subapical positioning of the centrosome plays a crucial role in OSM-, but not cAMP-mediated stimulation of apical bile canalicular lumen development in hepatic HepG2 cells.

Immunofluorescence microscopic analysis reveals that ~48% of the centrosomes in a typical HepG2 cell population contain detectable amounts of PKA-RIIα. This increases to ~65% ($p < 0.01$) in oncostatin M-treated cells, but not in db-cAMP-treated cells. The enhanced association of PKA-RIIα with centrosomes is a result of anchoring via AKAPs as expression of the PKA-RII-displacing peptide AKAP-IS (Alto *et al*., 2003), which reduced the anchoring of PKA-RIIα to centrosomes, prevents the stimulatory effect of OSM. A scrambled version of the peptide was without effect. The association and dissociation of PKA-RIIα from centrosomal AKAPs has been shown to be regulated by phosphorylation of PKA-RIIα in mitotic cells (Carlson *et al*., 2001). In our studies, however, changes in the expression level of the cyclin-dependent kinase inhibitor p27Kip1 (indicative for altered cell cycle progression) or electrophoretic mobility shifts (indicative for changes in PKA-RIIα phosphorylation status) were not observed in response to OSM. Furthermore, expression of the AKAP-IS peptide did not significantly alter the proliferation rate, mitotic index, or cell cycle phase distribution pattern of the cell culture. As a part of the underlying molecular mechanism, our data suggest that signaling through MEK and ERK2 downstream of OSM stimulation is involved in stimulating centrosomal anchoring of PKA-RIIα. Fluorescence microscopical examination of cells treated with OSM for 30 min or 4 h and subsequently processed for phospho-ERK1/2 immunolabeling did not reveal a clear association of ERK1/2 with centrosomes (our unpublished data), suggesting that ERK2 does not or only transiently acts at the centrosome. How MEK–ERK2-dependent anchoring of PKA-RIIα to centrosomal AKAPs is regulated at the molecular level thus requires further studies.

Most PKA-RIIα–recruiting centrosomes displayed a subapical position. The tethering of PKA-RIIα to centrosomes may serve to reinforce the subapical position of these centrosomes. Indeed, the stable expression of the AKAP-IS peptide results in a perinuclear position of most centrosomes. A scrambled version of the peptide was without effect. Whereas reduced centrosomal PKA-RIIα anchoring clearly affects the subapical position of the centrosome, our data show that subapical centrosome positioning is unaffected by two structurally distinct PKA inhibitors (H89 and KT5720), and, therefore, is likely to be unrelated to enzymatic PKA activity. Intriguingly, even though the displacement of PKA-RIIα from centrosomes is incomplete, the resulting effect on centrosome position is prominent, which may suggest that the quantity of anchored PKA-RIIα, possibly proportionate to other centrosome-anchored (regulatory) molecules, rather than the anchoring of PKA-RIIα as such, controls subapical centrosome positioning. The molecular mechanisms underlying the subapical positioning of (PKA-RIIα–positive) centrosomes in hepatocytes requires further studies. Cytoskeletal elements are likely to be involved in this, possibly involving intermediate (cytokeratin) filaments that have been reported to anchor centrosomes to the apical surface of intestinal epithelial Caco-2 cells (Salas, 1999).

Concomitant with the perinuclear positioning of the centrosome in cells expressing the PKA-displacing peptide, also the subcellular distribution of the CE/SAC shifted from the subapical to the perinuclear region. Interestingly, the sub-

apical localization of rab11a-positive ARE is preserved in cells expressing the AKAP-IS peptide, although an additional pool of rab11a was associated with the perinuclear centrosomes. These data indicate that common endosomes and apical recycling endosomes can be spatially separated, underscoring that these represent distinct entities (Brown *et al*., 2000; Leung *et al*., 2000; Wang *et al*., 2000). Whereas basolateral-to-apical membrane trafficking, i.e., transcytosis, in epithelial cells including hepatocytes involves sequential passage through an early endosome, common endosome, and apical recycling endosome (for review, see Tuma and Hubbard, 2003), the spatial separation of the latter two as observed in cells expressing the AKAP-IS peptide does not seem to impede constitutive or oncostatin M-stimulated transcytosis. Because the stimulatory effect of OSM on apical lumen development has been shown to require apical surface-directed membrane flow from common endosomes (van IJzendoorn *et al*., 2004a,b), the combined data suggest that apical surface-directed membrane trafficking is necessary but not sufficient for OSM-stimulated apical lumen development.

Importantly, the ERK2-mediated anchoring of PKA-RIIα at the centrosome and the concomitant subapical position of PKA-RIIα–positive centrosomes seems essential for OSM to stimulate apical bile canalicular lumen development, a process that was previously shown to require the enzymatic activity of PKA (van der Wouden *et al*., 2002). In fact, in AKAP-IS–expressing cells that show reduced centrosomal anchoring of PKA-RIIα and that are inhibited in their capability to position the centrosome subapically, oncostatin M decreases cell polarity, evidenced by a loss of apical lumens. Although the underlying mechanism for the decrease in cell polarity remains unknown, the data suggest that the ability of oncostatin M to stimulate the association of PKA-RIIα with centrosomes and the subcellular positioning of PKA-RIIα–positive centrosomes is vital for the outcome of the oncostatin M-elicited cellular response. We thus propose that OSM-stimulated anchoring of PKA-RIIα to centrosomes may serve to reinforce or stabilize the subapical position of the centrosome and that this is necessary for properly relaying the signals elicited by specific extracellular ligands such as OSM to subapically located effector molecules that participate in the development of bile canalicular lumens in manner that is uncoupled from lumen-directed trafficking. Strikingly, the inhibition of centrosomal PKA-RIIα anchoring and apical centrosome positioning in cells expressing the AKAP-IS peptide does not affect apical lumen development in unstimulated or in db-cAMP-stimulated cells. This implies that the regulated centrosomal anchoring of PKA-RIIα and subapical centrosome positioning is not essential for apical lumen development per se, but rather for apical lumen development in response to specific signaling molecules such as OSM. These data underscore that, in a single hepatic cell line (HepG2), multiple PKA-dependent signaling pathways operate in parallel in the process of polarity development and that centrosome-anchored PKA-RIIα and subapical centrosome positioning are important in some of these pathways.

ACKNOWLEDGMENTS

We thank J. Scott for providing the AKAP-IS and AKAP-scrambled constructs, J. Goldenring for the AKAP350 antibodies, and H. Kampinga (University Medical Center Groningen, Groningen, The Netherlands) for γ-tubulin antibodies. We thank D. Théard for the p27Kip1 expression experiment and valuable discussions. S.C.D.v.IJ. was supported by the Royal Duch Academy of Sciences (KNAW).

REFERENCES

Alto, N. M., Soderling, S. H., Hoshi, N., Langeberg, L. K., Fayos, R., Jennings, P. A., and Scott, J. D. (2003). Bioinformatic design of A-kinase anchoring protein-*in silico*: a potent and selective peptide antagonist of type II protein kinase A anchoring. Proc. Natl. Acad. Sci. USA *100*, 4445–4450.

Brown, P. S., Wang, E., Aroeti, B., Chapin, S. J., Mostov, K. E., and Dunn, K. W. (2000). Definition of distinct compartments in polarized Madin-Darby canine kidney (MDCK). cells for membrane-volume sorting, polarized sorting and apical recycling. Traffic *1*, 124–140.

Burakov, A., Nadezhdina, E., Slepchenko, B., and Rodionov, V. (2003). Centrosome positioning in interphase cells. J. Cell Biol. *162*, 963–969.

Buendia, B., Bre, M. H., Griffiths, G., and Karsenti, E. (1990). Cytoskeletal control of centrioles movement during the establishment of polarity in Madin-Darby canine kidney cells. J. Cell Biol. *110*, 1123–1135.

Carlson, C. R., Witczak, O., Vossebein, L., Labbé, J. C., Skálhegg, B. S., Keryer, G., Herberg, F. W., Collas, P., and Taskén, K. (2001). CDK1-mediated phosphorylation of the RIIα regulatory subunit of PKA works as a molecular switch that promotes dissociation of RIIα from centrosomes at mitosis. J. Cell Sci. *114*, 3243–3254.

Casanova, J. E., Wang, X., Kumar, R., Bhartur, S. G., Navarre, J., Woodrum, J. E., Altschuler, Y., Ray, G. S., and Goldenring, J. R. (1999). Association of Rab25 and Rab11a with the apical recycling system of polarized Madin-Darby canine kidney cells. Mol. Biol. Cell *10*, 47–61.

Cohen, D., Brennwald, P. J., Rodriguez-Boulan, E., and Musch, A. (2004). Mammalian PAR-1 determines epithelial lumen polarity by organizing the microtubule cytoskeleton. J. Cell Biol. *164*, 717–727.

Cowan, C. R., and Hyman, A. A. (2004). Centrosomes direct cell polarity independently of microtubule assembly in *C. elegans* embryos. Nature *431*, 92–96.

de Anda, F. C., Pollarolo, G., Da Silva, J. S., Camoletto, P., G., Feiguin, F., and Dotti, C. G. (2005). Centrosome localization determines neuronal polarity. Nature *436*, 704–708.

Diviani, D., and Scott, J. D. (2001). AKAP signaling complexes at the cytoskeleton J. Cell Sci. *114*, 1431–1437.

Doxsey, S. J., Stein, P., Evans, L., Calarco, P. D., and Kirschner, M. (1994). Pericentrin, a highly conserved centrosome protein involved in microtubule organization. Cell *76*, 639–650.

Dylewski, D. P., and Keenan, T. W. (1984). Centrioles in the mammary epithelium of the rat. J. Cell Sci. *72*, 185–193.

Gradilone, S. A., Garcia, F., Huebert, R. C., Tietz, P. S., Larocca, M. C., Kierbel, A., Carreras, F. I., Larusso, N. F., and Marinelli, R. A. (2003). Glucagon induces the plasma membrane insertion of functional aquaporin-8 water channels in isolated rat hepatocytes. Hepatology *37*, 1435–1441.

Grindstaff, K. K., Bacallao, R. L., and Nelson, W. J. (1998). Apiconuclear organization of microtubules does not specify protein delivery from the trans-Golgi network to different membrane domains in polarized epithelial cells. Mol. Biol. Cell *9*, 685–699.

Herrema, H., Czajkowska, D., Theard, D., van der Wouden, J. M., Kalicharan, D., Zolghadr, B., Hoekstra, D., and van Ijzendoorn, S. C. (2006). Rho kinase, myosin-II, and p42/44 MAPK control extracellular matrix-mediated apical bile canalicular lumen morphogenesis in HepG2 cells. Mol. Biol. Cell *17*, 3291–3303.

Higginbotham, H., Tanaka, T., Brinkman, B. C., and Gleeson, J. G. (2006). GSK3beta and PKCzeta function in centrosome localization and process stabilization during Slit-mediated neuronal repolarization. Mol. Cell Neurosci. *32*, 118–132.

Hobdy-Henderson, K. C., Hales, C. M., Lapierre, L. A., Cheney, R. E., and Goldenring, J. R. (2003). Dynamics of the apical plasma membrane recycling system during cell division. Traffic *4*, 681–893.

Hoekstra, D., Tyteca, D., and van Ijzendoorn, S. C. (2004). The subapical compartment: a traffic center in membrane polarity development. J. Cell Sci. *117*, 2183–2192.

Houliston, E., Pickering, S. J., and Maro, B. (1987). Redistribution of microtubules and pericentriolar material during the development of polarity in mouse blastomeres. J. Cell Biol. *104*, 1299–1308.

Kagawa, T., Varticovski, L., Sai, Y., and Arias, I. M. (2002). Mechanism by which cAMP activates PI3-kinase and increases bile acid secretion in WIF-B9 cells. Am. J. Physiol. *283*, 1655–1666.

Kamiya, A., Kinoshita, T., and Miyajima, A. (2001). Oncostatin M and hepatocyte growth factor induce hepatic maturation via distinct signaling pathways. FEBS Lett. *492*, 90–94.

Keryer, G., Luo, Z., Cavadore, J. C., Erlichman, J., and Bornens, M. (1993). Phosphorylation of the regulatory subunit of type II beta cAMP-dependent protein kinase by cyclin B/p34cdc2 kinase impairs its binding to microtubule-associated protein 2. Proc. Natl. Acad. Sci. USA *90*, 5418–5422.

Klausen, P., Pedersen, L., Jurlander, J., and Baumann, H. (2000). Oncostatin M and interleukin 6 inhibit cell cycle progression by prevention of p27kip1 degradation in HepG2 cells. Oncogene *19*, 3675–3683.

Kubitz, R., Huth, C., Schmitt, M., Horbach, A., Kullak-Ublick, G., and Haussinger, D. (2001). Protein kinase C-dependent distribution of the multidrug resistance protein 2 from the canalicular to the basolateral membrane in human HepG2 cells. Hepatology *34*, 340–350.

Kubitz, R., Sutfels, G., Kuhlkamp, T., Kolling, R., and Haussinger, D. (2004). Trafficking of the bile salt export pump from the Golgi to the canalicular membrane is regulated by the p38 MAP kinase. Gartroenterology *126*, 541–553.

Lange, B. M. (2002). Integration of the centrosome in cell cycle control, stress response and signal transduction pathways. Curr. Opin. Cell Biol. *14*, 35–43.

Leung, S. M., Ruiz, W. G., and Apodaca, G. (2000). Sorting of membrane and fluid at the apical pole of polarized Madin-Darby canine kidney cells. Mol. Biol. Cell *11*, 2131–2150.

Meads, T., and Schroer, T. A. (1995). Polarity and nucleation of microtubules in polarized epithelial cells. Cell Motil. Cytoskeleton *32*, 273–288.

Michel, J. J., and Scott, J. D. (2002). AKAP mediated signal transduction. Annu. Rev. Pharmacol. Toxicol. *42*, 235–257.

Misra, S., Ujhazy, P., Gatmaitan, Z., Varticovski, L., and Arias, I. M. (1998). The role of phosphoinositide 3-kinase in taurocholate-induced trafficking of ATP-dependent canalicular transporters in rat liver. J. Biol. Chem. *273*, 26638–26644.

Musch, A. (2004). Microtubule organization and function in epithelial cells. Traffic *5*, 1–9.

Perez, L. M., Milkiewicz, P., Ahmed-Choudhury, J., Elias, E., Ochoa, J. E., Sanchez Pozzi, E. J., Coleman, R., and Roma, M. G. (2006). Oxidative stress induces actin-cytoskeletal and tight-junctional alterations in hepatocytes by a Ca2+-dependent, PKC-mediated mechanism: protective effect of PKA. Free Radic. Biol. Med. *40*, 2005–2017.

Prekeris, R., Klumperman, J., and Scheller, R. H. (2000). A Rab11/Rip11 protein complex regulates apical membrane trafficking via recycling endosomes. Mol. Cell. *6*, 1437–1448.

Rizzolo, L. J., and Joshi, H. C. (1993). Apical orientation of the microtubule organizing center and associated gamma-tubulin during the polarization of the retinal pigment epithelium in vivo. Dev. Biol. *157*, 147–156.

Roma, M. G., Milkiewicz, P., Elias, E., and Coleman, R. (2000). Control by signaling modulators of the sorting of canalicular transporters in rat hepatocyte couplets: role of the cytoskeleton. Hepatology *32*, 1342–1356.

Roma, M. G., Stone, V., Shaw, R., and Coleman, R. (1998). Vasopressin-induced disruption of actin cytoskeletal organization and canalicular function in isolated rat hepatocyte couplets: possible involvement of protein kinase C. Hepatology. *28*, 1031–1041.

Sai, Y., Nies, A. T., and Arias, I. M. (1999). Bile acid secretion and direct targeting of mdr1-green fluorescent protein from Golgi to the canalicular membrane in polarized WIF-B cells. J. Cell Sci. *112*, 4535–4545.

Salas, P.J.I. (1999). Insoluble γ-tubulin-containing structures are anchored to the apical network of intermediate filaments in polarized CACO-2 epithelial cells. J. Cell Biol. *146*, 645–657.

Tuma, P. L., and Hubbard, A. L. (2003). Transcytosis: crossing cellular barriers. Physiol. Rev. *83*, 871–932.

Tuma, P. L., Nyasae, L. K., Backer, J. M., and Hubbard, A. L. (2001). Vps34p differentially regulates endocytosis from the apical and basolateral domains in polarized hepatic cells. J. Cell Biol. *154*, 1197–1208.

van der Wouden, J. M., van IJzendoorn, S. C., and Hoekstra, D. (2002). Oncostatin M regulates membrane traffic and stimulates bile canalicular membrane biogenesis in HepG2 cells. EMBO J. *21*, 6409–6418.

van IJzendoorn, S. C., and Hoekstra, D. (1999). Polarized sphingolipid transport from the subapical compartment: evidence for distinct sphingolipid domains. Mol. Biol. Cell *10*, 3449–3461.

van IJzendoorn, S. C., and Hoekstra, D. (1998). (Glyco)sphingolipids are sorted in sub-apical compartments in HepG2 cells: a role for non-Golgi-related intracellular sites in the polarized distribution of (glyco)sphingolipids. J. Cell Biol. *142*, 683–696.

van IJzendoorn, S. C., and Hoekstra, D. (2000). Polarized sphingolipid transport from the subapical compartment changes during cell polarity development. Mol. Biol. Cell *11*, 1093–1101.

van IJzendoorn, S. C., Theard, D., Van Der Wouden, J. M., Visser, W., Wojtal, K. A., and Hoekstra, D. (2004a). Oncostatin M-stimulated apical plasma membrane biogenesis requires p27(Kip1)-regulated cell cycle dynamics. Mol. Biol. Cell *15*, 4105–4114.

van IJzendoorn, S. C., Van Der Wouden, J. M., Liebisch, G., Schmitz, G., and Hoekstra, D. (2004b). Polarized membrane traffic and cell polarity development is dependent on dihydroceramide synthase-regulated sphinganine turnover. Mol. Biol. Cell *15*, 4115–4124.

van IJzendoorn, S. C., Zegers, M. M., Kok, J. W., and Hoekstra, D. (1997). Segregation of glucosylceramide and sphingomyelin occurs in the apical to basolateral transcytotic route in HepG2 cells. J. Cell Biol. *137*, 347–357.

Wald, F. A., Figueroa, Y., Oriolo, A. S., and Salas, P. J. (2003). Membrane repolarization is delayed in proximal tubules after ischemia-reperfusion: possible role of microtubule-organizing centers. Am. J. Physiol. *285*, 230–240.

Wang, E., Brown, P. S., Aroeti, B., Chapin, S. J., Mostov, K. E., and Dunn, K. W. (2000). Apical and basolateral endocytic pathways of MDCK cells meet in acidic common endosomes distinct from a nearly-neutral apical recycling endosome. Traffic *1*, 480–493.

Wojtal, K. A., de Vries, E., Hoekstra, D., and van IJzendoorn, S. C. (2006). Efficient trafficking of MDR1/P-glycoprotein to apical canalicular plasma membranes in HepG2 cells requires PKA-RIIalpha anchoring and glucosylceramide. Mol. Biol. Cell *17*, 3638–3650.

Zegers, M. M., and Hoekstra, D. (1997). Sphingolipid transport to the apical plasma membrane domain in human hepatoma cells is controlled by PKC and PKA activity: a correlation with cell polarity in HepG2 cells. J. Cell Biol. *138*, 307–321.

Zegers, M. M., Kok, J. W., and Hoekstra, D. (1997). Use of photoactivatable sphingolipid analogues to monitor lipid transport in mammalian cells. Biochem. J. *328*, 489–498.

Zeligs, J. D. (1979). Association of centrioles with clusters of apical vesicles in mitotic thyroid epithelial cells. Are centrioles involved in directing secretion? Cell Tissue Res. *201*, 11–21.